Electronic Supplementary Material (ESI) for Environmental Science: Nano.

Supporting Information

Towards validation of the NanoDUFLOW nanoparticle fate model for the river Dommel, The Netherlands

Jeroen J.M. de Klein[1], Joris T.K Quik[1,2], Patrick Bauerlein[3], Albert A. Koelmans[1,4,*]

[1] Aquatic Ecology and Water Quality Management Group, Department of Environmental Sciences, Wageningen University, P.O. Box 47, 6700 AA Wageningen, The Netherlands.

[2] National Institute of Public Health and the Environment, Centre for Safety of Products and Substances, Bilthoven, the Netherlands.

[3] KWR Watercycle Research Institute, Groningenhaven 7, 3433 PE Nieuwegein, The Netherlands.

[4] IMARES – Institute for Marine Resources & Ecosystem Studies, Wageningen UR, P.O. Box 68, 1970 AB IJmuiden, The Netherlands.

***Corresponding Author**
E-mail: Bart.Koelmans@wur.nl, Telephone: +31 317 483 201

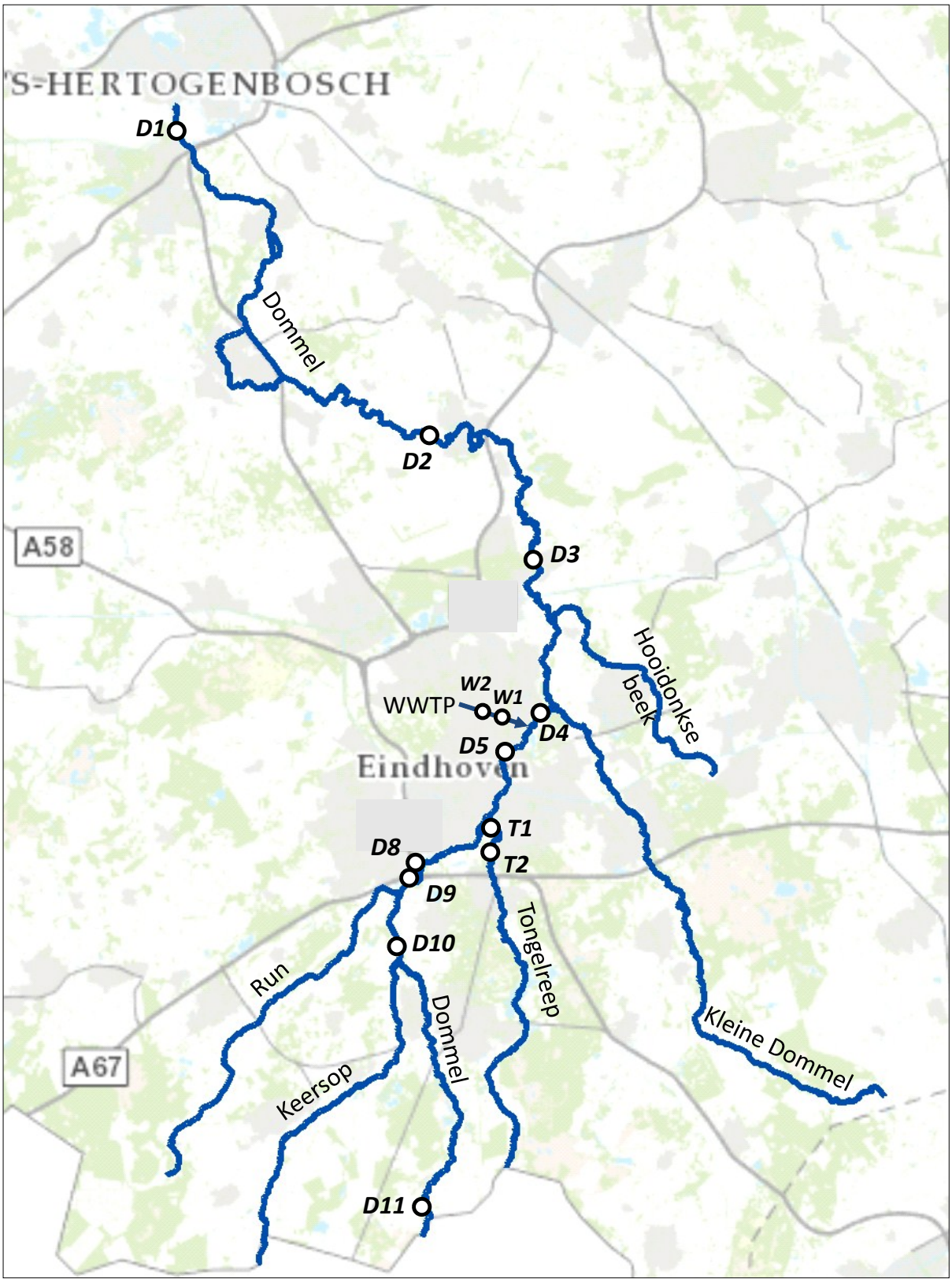

Figure S1. Map of the Dommel river area and the sampling locations (for location ID see Table S5).

Table S1. Characteristics of the NanoDUFLOW model implemented for river Dommel.

Total model river length	40.3 km
Discharge, min – max (avg.)	1.02 - 5.38 (3.29) $m^3 s^{-1}$
Flow velocity, min – max (avg.)	0.00355- 0.536 (0.318) m s^{-1}
Section width, min - max	8 – 228 m
Number of calculation sections	471
Average section length	87.7 m

Table S2. Boundary conditions for the NanoDUFLOW model implemented for river Dommel.[a]

	Q inflow	Ce	Al	Ti	Zr
	$m^3 s^{-1}$	$\mu g l^{-1}$	$\mu g l^{-1}$	$\mu g l^{-1}$	$\mu g l^{-1}$
Upstream Dommel	1.58	0.270	5.94	0.680	0.074
Effluent WWTP	1.70	0.102	3.18	0.843	0.033
Tongelreep	1.19	0.096	2.20	0.637	0.104
Keersop	0.55	0.096	2.20	0.637	0.104
Run	0.28	0.096	2.20	0.637	0.104
Hooidonkse Beek	0.13	0.096	2.20	0.637	0.104
Kleine Dommel	1.65	0.096	2.20	0.637	0.104

[a] 'Q inflow' is volume of water per unit of time flowing into the main Dommel river. Elemental concentrations for Ce, Al, Ti, Zr relate to measurements with Asymmetric Flow-Field-Flow Fractionation (AF4).

Table S3. Densities of the oxides selected to represent ENP oxides.[a,b]

	CeO_2	$Al(OH)_3$	TiO_2	ZrO_2
Densities ENP oxides (g cm^{-3})	7.65	2.42	4.23	5.68

a) Weast, R.C. and Astle, M.J. (eds) (1980) Handbook of Chemistry and Physics, CRC Press, Inc, Boca Raton, Florida.
b) Due to the overwhelming effect of natural colloid density on overall heteroaggregate density, model output was not sensitive to variations among mineral densities per element.

Table S4. Initial conditions of suspended solids (SS) number concentration per size class, in the water column and the top 10 cm of the sediment.

	Class	**SS water**	**SS sediment**
Concentration	1	3378	0
(10^9 L^{-1})	2	125.1	24936.43
	3	3.38	2244.27
	4	0.125	249.36
	5	0	22.44
	Sum	3506.91	27452.52

Table S5. Metal concentrations as measured with Asymmetric Flow-Field-Flow Fractionation (AF4) in < 450 nm filtered water samples, taken from the river Dommel in May 2013, detection limits and average and range of relative standard deviations of triplicate measurements.

ID	Location	Distance km	Ce µg l^{-1}	Al µg l^{-1}	Ti µg l^{-1}	Zr µg l^{-1}
D11	Dommel11	0	0.270	5.939	0.680	0.074
D10	Dommel10	12.0	0.210	5.132	0.673	0.079
D9	Dommel9	14.3	0.188	5.674	0.675	0.089
D8	Dommel8	14.8	0.153	4.473	0.683	0.108
D5	Dommel5	22.1	0.099	3.574	0.652	0.089
D4	Dommel4	23.7	0.091	2.836	0.698	0.089
D3	Dommel3	31.2	0.097	4.245	0.896	0.131
D2	Dommel2	39.9	0.082	4.546	1.150	0.129
D1	Dommel1	63.5	0.108	4.546	1.049	0.227
T1	Tongelreep1		0.087	2.189	0.648	0.099
T2	Tongelreep2		0.105	2.206	0.626	0.108
W1	Influent WWTP		0.329	13.653	9.457	0.177
W2	Effluent WWTP		0.102	3.185	0.843	0.033
Detection limit			0.005	0.5	0.1	0.03
Average %RSD[1]			2.35	3.94	4.6	2.56
Minimum %RSD[2]			1.11	1.89	0.28	0.88
Maximum %RSD[3]			4.87	5.18	7.39	4.86

[1] average relative standard deviation in triplicate AF4 ICP-MS measurements per sample

[2] minimum relative standard deviation in triplicate AF4 ICP-MS measurements per sample

[3] maximum relative standard deviation in triplicate AF4 ICP-MS measurements per sample

NanoDUFLOW Model description

This section provides an extended overview of process descriptions for NanoDUFLOW. The description is based on Quik et al. (2015) and updated to represent the model implementation features of the present study. References are provided for more background and detail. Parameter values are listed and motivated in a separate table (Table S6).

Transformation processes

Homoaggregation

Homoaggregation is the process where ENPs interact with each other to form aggregates. The aggregation rate constant is the product of the frequency of collisions between ENPs (K) and the attachment efficiency (α). Homoaggregation can be quantitatively described by the von Smoluchowski equation (1917), which has been recommended for modeling the fate of ENPs in natural waters (Lyklema 2005, Arvidsson et al. 2011, Quik et al. 2014b):

$$\frac{dn_j}{dt} = \frac{1}{2}\sum_{i=1}^{i=j-1} \alpha_{i,j-1} K_{i,j-i} n_i n_{j-i} - n_j \sum_{i=1}^{i=\infty} \alpha_{i,j} K_{i,j} n_i \qquad \text{(Eq. S1)}$$

n_j Particle number concentration of size class j [G# m^{-3}] in giga particles (10^9).

t Time [s]

$\alpha_{i,j}$ Attachment efficiency of particle i with j [-]

$K_{i,j}$ Collision frequency of particle i with j [m^3 G#$^{-1}$ s^{-1}]

The collision frequency ($K_{i,j}$) is given by:

$$K_{i,j} = \left(\frac{2k_bT}{3\mu}\frac{(a_i+a_j)^2}{a_ia_j} + \frac{4}{3}G(a_i+a_j)^3 + \left(\frac{2\pi g}{9\mu}\right)(\rho_p-\rho_w)(a_i+a_j)(a_i-a_j)\right)10^9 \qquad \text{(Eq. S2)}$$

k_b Boltzman constant [m^2 kg s^{-2} K^{-1}]

T Temperature [K]

μ Viscosity [kg s^{-1} m^{-1}]

a Particle radius [m]

G Shear rate [s^{-1}] (calculated from Duflow flow rate, see Table S6, Eq S21)

g Gravitation acceleration [m s^{-2}]

ρ_p Density of the particle [kg m^{-3}]

ρ_w Density of the suspending medium [kg m^{-3}]

Homoaggregation is implemented in DUFLOW as follows. Five size classes of ENPs are considered, which grow from one class to the next, and are corrected for the difference in mass of the two size classes (Eq S3).

This leads to the following simplification of equation 1:

$$\frac{dn_j}{dt} = -\frac{1}{2}\alpha_{hom} K_{j,j} n_j n_j + \frac{1}{2}\alpha_{hom} K_{i,i} n_i n_i \frac{\rho_i a_i^3}{\rho_j a_j^3} \qquad \text{with i = j-1} \qquad \text{(Eq. S3)}$$

Where the second term in Eq 3 is zero for j=1.

This simplification implies that ENP removal due to subsequent interactions of homo-aggregates with primary ENPs and ENP homo-aggregates from other size classes is assumed to be negligible, which is based on the extremely fast initial removal of these primary ENPs due to homo- and hetero-aggregation. In our recent study we used a full Smoluchowski model (i.e. Eq S1) and already showed that sedimentation due to homoaggregation is negligible at low ENP concentrations (e.g. 10 µg L^{-1} CeO_2 ENPs) (Quik et al. 2014b). In order to test if this is also true for the present simplified homoaggregation implementation (Eq. S3), Quik et al. (2015) performed two different model simulations: (i) with α_{hom}=0 and (ii) with α_{hom}=1 (i.e. minimizing and maximizing the role of homoaggregation, respectively) for the highest modelled ENP concentration (100 ng/L CeO_2). This resulted in no discernible difference in the concentration profile (Figure S1.1). This implies that the simplification in Eq. S3 does not affect the model scenarios calculations in the present paper and thus that the assumption is valid.

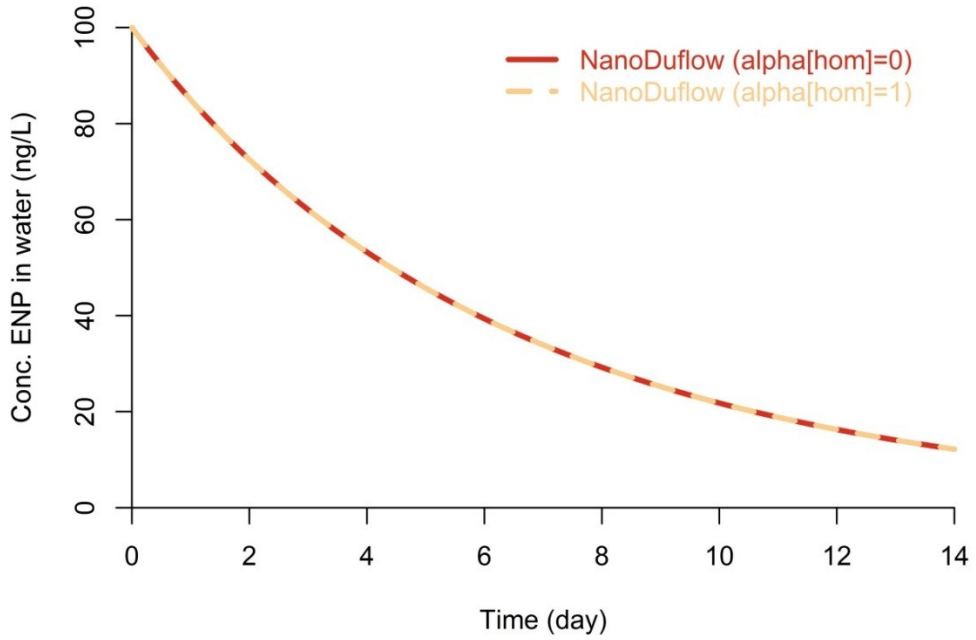

Figure S1.1. Concentration of engineered CeO_2 nanoparticles (ENPs) in water with initial concentration of 100 ng/L CeO_2 ENPs using Eq. S3 and Eq. S8 using 5 size categories). Solid line depicts α_{hom}=0 and dashed line α_{hom}=1. From Quik et al (2015).

Heteroaggregation

Heteroaggregation is the process where ENPs interact with natural suspended solids (SS) to form an aggregate or agglomerate. The quantitative description of heteroaggregation is based on the same principles as homoaggregation, where the attachment efficiency combined with the collision frequency make up the rate of change in heteroaggregate concentrations. For ENPs this is given by (Lyklema 2005, Arvidsson et al. 2011, Praetorius et al. 2012, Meesters et al. 2014):

$$\frac{dn_j}{dt} = -\alpha_{hetero} n_j \sum_{1}^{i} K_{j,SSi}\, n_{SSi} \qquad \text{(Eq. S4)}$$

Where n is the number of size classes of SS and $K_{j,SSj}$ is given by (Lyklema, 2005):

$$K_{j,SSi} = \left(\frac{2k_b T}{3\mu} \frac{(a_j + a_{SSi})^2}{a_j a_{SSi}} + \frac{4}{3} G (a_j + a_{SSi})^3 + \pi (a_j + a_{SSi})^2 |v_{s,j} - v_{s,SSi}| \right) 10^9 \qquad \text{(Eq. S5)}$$

G in the term for orthokinetic aggregation is calculated from the flow rate as calculated by the DUFLOW hydrological model, thus providing a direct link between river hydrodynamics, hydrology and aggregation behavior (river hydrodynamics→ flow velocity→ shear→ orthokinetic aggregation → collision frequency→ heteroaggregation rate), see Table S6, Eq S21.

Surface modification

The surfaces of pristine nanoparticles are supposed to be modified by natural organic matter such as humic acid and fulvic acid. Particles are repelled from each other by an electric charge on the particle surface, i.e. electrostatic repulsion. Aggregation can also be limited by a physical barrier formed by large organic molecules, which is referred to as steric hindering. In NanoDUFLOW these issues are implicitly accounted for by assigning a conditional attachment efficiency (α) which scales between 0 and 1.

Following Praetorius et al (2012), our scenario calculations used a constant attachment efficiency for homoaggregation and for heteroaggregation (α_{hom} and α_{het}).

Dissolution and degradation

Dissolution refers to the transformation of metal particles to dissolved metal ions. Dissolution is quantified using a first order removal rate k_{dis} as previously used by several studies (Praetorius et al. 2012, Meesters et al. 2014, Quik et al. 2011).

$$\frac{dn_j}{dt} = -k_{dis}\, n_j \qquad \text{(Eq S6)}$$

k_{diss}: Dissolution rate constant

In order to take into account processes, other than dissolution, that transform the ENPs, such as transformation of Silver ENPs to Silver sulfide (Ag_2S) particles, a degradation term is introduced using a first order removal rate, k_{deg}.

$$\frac{dn_j}{dt} = -k_{deg} n_j \qquad \text{(Eq S7)}$$

k_{deg}: Degradation rate constant

General

Most of these transformation processes take place in the water phase, although degradation and dissolution occur in the sediment as well. Furthermore, heteroaggregation also occurs in the sediment when homoaggregates settle to the sediment. ENPs that have entered the sediment are assumed not to remain as non-attached single ENP or ENP homoaggregates in the sediment phase. Because of the very high collision frequency between ENPs and SSs upon ENPs reaching the sediment, they can be assumed to be converted to heteroaggregates, contrary to the water phase where the collision frequency is more limited. Note that in the present study the concentrations in sediment were not simulated.

Transport processes

Sedimentation

Sedimentation is the transport of ENPs or SSs from the water column to the sediment by gravitation. Separate sedimentation rates are calculated for each ENP class, SS class or heteroaggregate class. The sedimentation rate is calculated using Stokes law, (Stokes 1850) assuming that the particles on average are spherical (Lyklema, 2005).

$$\frac{dn_j}{dt} = -\frac{v_s}{d} n_j \qquad \text{(Eq S8)}$$

d Sedimentation length [m]

v_s Sedimentation rate [m s^{-1}]

The sedimentation rate (v_s) can be calculated with:

$$v_s = \frac{2a_j^2(\rho_p - \rho_w)g}{9\mu} \qquad \text{(Eq S9)}$$

Sedimentation rates for ENP-SS heteroaggregates are calculated based on an average size and density, as calculated based on the size and density of the SS and ENP in the heteroaggregate.

Sediment transport

Lateral transport of sediment is modeled as resuspension/sedimentation and lateral sediment transport in the water column (Blom and Aalderink 1998, Brouwer 2012).

Burial to deeper sediment layers

In case of net sedimentation, burial from the mixed sediment top layer is modeled as a first order loss process (Koelmans et al. 2009). The top sediment layer of 10 cm is assumed to be available for resuspension. Due to burial this layer is converted to more compact deeper sediment layers. This results in burial of the incorporated nanoparticle heteroaggregates to these deeper sediment layers.

Sediment burial is quantified using first order kinetics:

$$\frac{dn_j}{dt} = - k_{bur} n_j \qquad \text{(Eq S10)}$$

Resuspension

Resuspension is described using a critical shear stress level below which resuspension does not occur according to the equations of Partheniades, which applies for the suspended load transport (Blom and Aalderink 1998). When the critical shear stress (τ_{crit}) is exceeded, a resuspension flux (R_j) is calculated based on the ratio between the actual and the critical shear stress and a resuspension rate constant.

$$R_j = R_{jmax}\left(\frac{\tau}{\tau_{crit}} - 1\right) \qquad \text{(Eq. S11)}$$

in which $\tau = \rho_w\left(\frac{g^{0.5} v_w}{Chezy}\right)^2$ [Pa] (Eq. S12)

R_{jmax}: Maximum resuspension constant for SS or SS-ENP j [G# m^{-2} s^{-1}]

v_w: flow rate of water obtained from Duflow [m s^{-1}]

Chezy: Chezycoefficient [$m^{0.5}$ s^{-1}]

Advection

Advection is implemented using DUFLOW Modeling Studio (v3.8.7) which is a software package for one-dimensional unsteady flow in open-channel systems (Clemmens et al. 1993, Aalderink et al. 1996). Water levels and flow rates are determined by solving the St. Venant equations of continuity and momentum with the Preissmann scheme, using initial and boundary conditions, such as an incoming flow at the upstream part of the model and a fixed downstream water level. DUFLOW calculates discharge, water level and mean velocity for each section and for each time step. Chemical transport is modelled by solving the advection-diffusion equation simultaneously with the hydrology for all network sections.

State variables

The state of i classes of ENPs and j classes of SS and all i x j combinations of ENP-SS heteroaggregates are accounted for using the above mentioned processes. This is done in the water and sediment compartment with i =5 and j=5.

Rate equations:

This results in the following overall mass balance equation for ENPs in water:

$$\frac{dn_i}{dt} = n_i\left(- \alpha_{hetero} \sum_{1}^{j} (K_{i,j}\, n_j) - \frac{v_{s,i}}{d} - k_{dis,i} - \frac{1}{2}\, \alpha_{hom} K_{i,i}\, n_i \right) + \frac{1}{2} \alpha_{hom}\, K_{i-1,i-1}\, n_{i-1} n_{i-1} \frac{\rho_{i-1} a_{i-1}^{3}}{\rho_i a_i^3}$$

(Eq S13)

The mass balance equation for suspended solids in water reads:

$$\frac{dn_j}{dt} = n_j\left(- \alpha_{hetero} \sum_{1}^{i} (K_{i,j}\, n_i) - \frac{v_{s,j}}{d} \right) + {R_j}/{d}$$

(Eq S14)

And for heteroaggregates in water:

$$\frac{dn_{i,j}}{dt} = - n_{i,j}\left(\frac{v_{s,ij}}{d} + k_{dis,i} \right) + \alpha_{hetero} K_{i,j} n_i n_j + {R_{i,j}}/{d}$$

(Eq S15)

Engineered nanoparticles which are removed from the water phase due to direct sedimentation are also accounted for, but are assumed to be transformed to heteroaggregates instantaneously upon arrival in in the sediment.

$$\frac{dn_{s,i}}{dt} = n_i v_{s,i}$$

(Eq. S16)

The mass balance for the sedimented (formerly suspended) solids present in the sediment

$$\frac{dn_{s,j}}{dt} = n_j v_{s,j} - n_{sj} k_{bur,j} - F_{ENP,SSj} \sum_{i} (v_{s,i} n_i) - R_j$$

(Eq. S17)

Where $F_{ENP,SSj}$ is:

$$F_{npNCj} = \frac{n_j}{\sum_{1}^{j} n_j}$$

(Eq. S18)

The mass balance for heteroaggregates present in sediment is:

$$\frac{dn_{s,i,j}}{dt} = n_{i,j} v_{s,i,j} + n_i v_{s,i} F_{ENPSSj} - n_{s,i,j}(k_{deg,ENPj} + k_{bur,ENPj}) - R_{i,j}$$

(Eq. S19)

Parameters

Table S6. NanoDuflow model parameters

Parameter	Description	Default	Source and additional info.
k_{bolz}	Bolzman constant	1.3806488 × 10^{-23} m^2 kg s^{-2} K^{-1}	
g	Gravitational acceleration	9.81 m s^{-2}	
μ	Viscosity of suspending medium	0.0012552 kg s^{-1} m^{-1}	Viscosity of water at 11.7 °C (Weast and Astle 1980)
ρ_w	Density of suspending medium	999.447 kg m^{-3}	Density of water at 11.7 °C (Weast and Astle 1980)
T	Temperature of suspending medium	284.7 K	10 year average water temperature of the Dommel. (2000-2010)(Waterboard De Dommel 2012)
Chezy	Chezy coefficient	40 $m^{0.5}$ s^{-1}	As used in the hydrological model of the Dommel.(Brouwer 2012, Langeveld et al. 2013)
ρ_{pr}	Density of primary particle	*See table S3.*	Bulk density (Weast and Astle 1980)
a_{pr}	Radius of primary particle	ENP: 10 nm	Default value for ENPs in Quik et al (Quik et al. 2014a). Due to fast heteroaggregation with much larger natural colloids, the model output was not sensitive to initial size.
Df	Fractal dimension ENP homoaggregates	2.5	ENP, i.e. CeO_2 aggregates where shown to be fairly compact resulting in a best guess of 2.5.
α_{hom}	Attachment efficiency homoaggregation	0.5	Default value based on measurements by Keller et al. (2010) in natural surface waters (α_{hom} = 0.5 for CeO_2 ENPs in Santa Clara river water).
α_{het}	Attachment efficiency heteroaggregation	0.5	Default value based on measurements by Keller et al. (2010) in natural surface waters (α_{hom} = 0.5 for CeO_2 ENPs in Santa Clara river water). The effect of the magnitude of α_{het} between 0.1 and 1 on simulation results was tested.
a_{ENPj}	Radius of ENP homoaggregate i	j=1: 30 nm, j=2: 75 nm, j=3: 150 nm, j=4: 300 nm, j=5: 600 nm	5 size classes used for ENPs oxides. Based on the size distributions measured using Nanoparticle Tracking Analysis which reported sizes ranging from ~15 nm up to 2000 nm after 1 day in filtered Rhine water (Quik et al. 2014a).
ρ_{ENPj}	Density of ENP homoaggregates i	$\rho_{npj} = \frac{\left(\left(\frac{a_{npj}}{a_{pr}}\right)^{Df} 4/3 \pi a_{pr}^3 \rho_{pr} + \rho_w \left(4/3 \pi a_{npj}^3 - \left(\frac{a_{npj}}{a_{pr}}\right)^{Df} 4/3 \pi a_{pr}^3 \rho_{pr}\right)\right)}{\left(4/3 \pi a_{npj}^3\right)}$ [kg m^{-3}] (Eq. S20)	
a_{ncj}	Radius of SS j	j=1: 0.5 µm j=2: 1.5 µm j=3: 5.0 µm j=4: 15 µm j=5: 50 µm	
ρ_{ncj}	Density of SS j	2120 kg m^{-3}	Density calculated from organic and inorganic content of suspended solids from 10 locations in the Dommel using the method by Boyd (Boyd 1995), where the fraction organic matter has a density of 1250 kg m^{-3} and the inorganic fraction has a density of

			2700 kg m^{-3} (Quik et al, 2015).
F_{aqsed}	Fraction water in sediment	0.7	From MacLeod et al. (2002).
τ_{critj}	Critical shear stress for resuspension of SS j	0.5 Pa	Value specifically measured for the Dommel river by L. Brouwer (2012).
v_w	Water flow rate	From hydrologic model results	
G	Shear rate	$G = 0.5\frac{g^{0.5} v_w}{Chezy\ \mu}$ [s^{-1}] (Eq. S21)	
R_{jmax}	Maximum resuspension constant for SS j	100 g m^{-2} day^{-1}	Converted to m^{-2} s^{-1} based on the SS radius and density. L. Brouwer (Brouwer 2012).
k_{disi}	Dissolution rate for ENP i in water	Virtually 0 s^{-1}	Negligible given the time scale of the simulation.
k_{degi}	Degradation rate for ENP i in sediment	Virtually 0 s^{-1}	Negligible given the time scale of the simulation.
k_{buri}	Sediment burial rate for ENP i	3.17 x 10^{-9} s^{-1}	From Koelmans et al (Koelmans et al. 2009)
$v_{s,i,j}$	Sedimentation rate of heteroaggregates	$v_{s,i,j} = \frac{\left(2g\left(a_i^{\,3} + a_j^{\,3}\right)^{2/3}\left(\frac{\rho_j\,{}^{4}\!/_{3}\,\pi\, a_j^3 + \rho_j\,{}^{4}\!/_{3}\,\pi\, a_i^3}{{}^{4}\!/_{3}\,\pi\, a_j^3 + {}^{4}\!/_{3}\,\pi\, a_i^3} - \rho_w\right)\right)}{9\mu}$ [m s^{-1}] (Eq. S22)	

Supporting Information References

Aalderink, R.H., Zoeteman, A. and Jovin, R. (1996) Effect of input uncertainties upon scenario predictions for the river Vecht. Water Science and Technology 33, 107-118.

Arvidsson, R., Molander, S., Sandén, B.A. and Hassellov, M. (2011) Challenges in Exposure Modeling of Nanoparticles in Aquatic Environments. Human and Ecological Risk Assessment 17(1), 245-262.

Blom, G. and Aalderink, R.H. (1998) Calibration of three resuspension/sedimentation models. Water Science and Technology 37(3), 41-49.

Boyd, C.E. (1995) Bottom Soils, Sediment, and Pond Aquaculture, Chapman & Hall, New York.

Brouwer, L. (2012) Obtaining a clear view: Sediment dynamics of river de Dommel and the possible consequences of suspended solids on the underwater light climate, Wageningen University, Wageningen.

Clemmens, A., Holly, F.J. and Schuurmans, W. (1993) Description and Evaluation of Program: Duflow. Journal of Irrigation and Drainage Engineering 119(Special Issue: Canal System Hydraulic Modeling), 724–734.

Filella, M. (2007) Environmental Colloids and Particles: behaviour, separation, and characterisation. Wilkinson, K.J. and Lead, J.R. (eds), Wiley.

Keller, A.A., Wang, H., Zhou, D., Lenihan, H.S., Cherr, G., Cardinale, B.J., Miller, R. and Ji, Z. (2010) Stability and Aggregation of Metal Oxide Nanoparticles in Natural Aqueous Matrices. Environmental Science & Technology 44(6), 1962-1967.

Koelmans, A.A., Nowack, B. and Wiesner, M.R. (2009) Comparison of manufactured and black carbon nanoparticle concentrations in aquatic sediments. Environ Pollut 157(4), 1110-1116.

Kolkman, A., Emke, E., Bäuerlein, P.S., Carboni, A., Tran, D.T., ter Laak, T.L., van Wezel, A.P. and de Voogt, P. (2013) Analysis of (Functionalized) Fullerenes in Water Samples by Liquid Chromatography Coupled to High-Resolution Mass Spectrometry. Anal Chem 85(12), 5867-5874.

Langeveld, J., Nopens, I., Schilperoort, R., Benedetti, L., Klein, J.J.M.d., Amerlinck, Y. and Weijers, S. (2013) On data requirements for calibration of integrated models for urban water systems. Water Science and Technology 68(3), 728-736.

Lyklema, J. (2005) Fundamentals of Interface and Colloid Science, Volume IV, Particulate Colloids. Lyklema, J. (ed), Elsevier Academic Press, Amsterdam.

MacLeod, M., Fraser, A.J. and Mackay, D. (2002) Evaluating and expressing the propagation of uncertainty in chemical fate and bioaccumulation models. Environmental Toxicology and Chemistry 21(4), 700-709.

Meesters, J.A.J., Koelmans, A.A., Quik, J.T.K., Hendriks, A.J. and van de Meent, D. (2014) Multimedia Modeling of Engineered Nanoparticles with SimpleBox4nano: Model Definition and Evaluation. Environmental Science & Technology 48(10), 5726-5736.

Praetorius, A., Scheringer, M. and Hungerbühler, K. (2012) Development of environmental fate models for engineered nanoparticles - a case study of TiO2 nanoparticles in the Rhine River. Environmental Science & Technology 46(12), 6705-6713.

Quik, J.T.K., Vonk, J.A., Hansen, S.F., Baun, A. and Van De Meent, D. (2011) How to assess exposure of aquatic organisms to manufactured nanoparticles? Environment International 37, 1068-1077.

Quik, J.T.K., Velzeboer, I., Wouterse, M., Koelmans, A.A. and Meent, D.v.d. (2014a) Heteroaggregation and sedimentation rates for nanomaterials in natural waters. Water Research 48, 169-179.

Quik, J.T.K., Van De Meent, D. and Koelmans, A.A. (2014b) Simplifying modeling of nanoparticle aggregation-sedimentation behavior in environmental systems: A theoretical analysis. Water Research 62C, 193-201.

Quik, J.T.K., J.J.M. de Klein, A.A. Koelmans. 2015. Spatially explicit fate modelling of nanomaterials in natural waters. Water Research, 80, 200-208.

Stokes, G.G. (1850) On the effect of the internal friction of fluids on the motion of pendulums. Transactions of the Cambridge Philosophical Society IX, 8.

Von Smoluchowski, M. (1917) Versuch einer mathematischen Theorie der Koagulationskinetik kolloider Lösungen. Zeitschrift fuer physikalische Chemie 92, 129 - 168.

Waterboard De Dommel (2012) Routine measurements water quality 2000-2010, http://www.dommel.nl.

Weast, R.C. and Astle, M.J. (eds) (1980) Handbook of Chemistry and Physics, CRC Press, Inc, Boca Raton, Florida.